Dicyanomethylene-Functionalized Squaraine as a Highly Selective Probe for Parallel G-Quadruplexes

ARTICLE *in* ANALYTICAL CHEMISTRY · JUNE 2014

Impact Factor: 5.64 · DOI: 10.1021/ac501619v · Source: PubMed

8 AUTHORS, INCLUDING:

Bing Jin
Nanjing Agricultural University
5 PUBLICATIONS **64** CITATIONS
SEE PROFILE

Nan Zhang
Chinese Academy of Sciences
14 PUBLICATIONS **154** CITATIONS
SEE PROFILE

Fuyi Wang
Chinese Academy of Sciences
67 PUBLICATIONS **1,342** CITATIONS
SEE PROFILE

Dihua Shangguan
Chinese Academy of Sciences
92 PUBLICATIONS **3,852** CITATIONS
SEE PROFILE

analytical chemistry

Article

pubs.acs.org/ac

Dicyanomethylene-Functionalized Squaraine as a Highly Selective Probe for Parallel G-Quadruplexes

Bing Jin,[†,‡] Xin Zhang,[†,‡] Wei Zheng,[†,‡] Xiangjun Liu,[†] Jin Zhou,[†,‡] Nan Zhang,[†,‡] Fuyi Wang,[†] and Dihua Shangguan*[,†]

[†]Beijing National Laboratory for Molecular Sciences, Key Laboratory of Analytical Chemistry for Living Biosystems, Institute of Chemistry, Chinese Academy of Sciences, Beijing, 100190, China

[‡]University of Chinese Academy of Sciences, Beijing 100049, China

Supporting Information

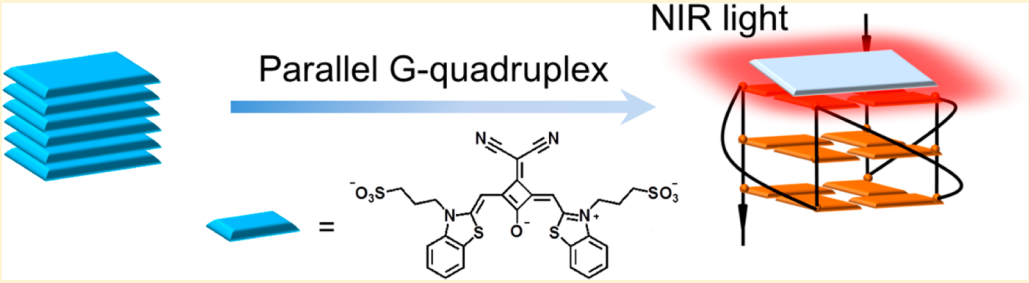

ABSTRACT: DNA sequences that can form G-quadruplexes (G4s) are highly prevalent in the genome. However, the structures and functions of most G4-forming sequences in the genome are poorly understood. Therefore, the development of molecular probes for G4 recognition in biological samples, especially probes with long wavelength, are important for the basic research of G4s. Squaraines dyes exhibit sharp and intense absorption and strong emission in the red to NIR region, but very few of them have been reported as probes for the recognition of nucleic acids. Here we report the interactions of two squaraine dyes, STS and CSTS, with different kinds of DNA. The dicyanomethylene-functionalized squaraine dye, CSTS, exhibits strong interaction with the parallel G4s, but no interaction with other DNA. In aqueous conditions, this interaction causes the transformation of CSTS from H-aggregates to monomers, which results in decline and growth of the absorption spectra of both forms. The parallel G4s enhance the fluorescence of both STS and CSTS, but the fluorescence enhancement of CSTS is much higher than that of STS. CSTS is demonstrated to bind to G4s through end-stacking model on G-quartet surface. The high selectivity of CSTS to parallel G4s is attributed to its V-shaped rigid planar π scaffold. The high selectivity, very low background fluorescence, large absorption coefficient, and high fluorescence quantum yield make CSTS hold great promise as a long-wavelength probe for parallel G4 detection in biological samples or in vivo.

Nucleic acids with repetitive guanine-rich sequences can fold into a four-stranded G-quadruplexes (G4s) structure, which are composed of multilayered stack of planar G-quartets via eight Hoogsteen hydrogen bonds.[1] Recently, G4s have attracted intensive investigation because of their important biological functions and their applications in supramolecular chemistry and nanotechnology.[2] A huge number of putative G-quadruplex-forming sequences (PQS) have been revealed in human genes, especially in promoter regions of oncogenes and telomere ends,[3] as well as in particular RNA domains, such as the first introns, 5′- and 3′-untranslated regions and telomeric RNA.[4,5] Besides being involved in telomere maintenance,[6] G4 structures have been found to play important roles in regulating the expression of many genes, such as c-myc,[7] c-kit,[8] KRAS,[9] VEGF,[10] c-myb,[11] and ILPR (insulin gene).[12] Therefore, G4s in gene are becoming promising targets for drug discovery.[13,14] In vivo, PQSs are embedded in double-stranded genome except for the single-stranded telomeric 3′-overhang, the G4 formation is suggested to occur transitorily during the processes, such as transcription, replication, and recombination, when the double-stranded DNA is actively denatured.[15] G4s are structurally polymorphic, which can be classified as parallel, antiparallel, and mixed parallel/antiparallel structures based on the orientation of the G-tracts in the quartet core. The folding topologies of G4s depend on the sequences, the loop geometry, and the local environment (such as ions, ligands or binding proteins).[1] Recently, DNA G4s and RNA G4s have been observed in human cells using G4 structure-specific antibody.[16,17] However, the G4 research in vivo is still at an early stage, the structures and functions of most PQSs in cells are poorly understood.[18] Therefore, the development of small-molecule fluorescent probes for G4s with specific structure is important for the basic research of G4s.

Received: April 21, 2014
Accepted: June 18, 2014

   dx.doi.org/10.1021/ac501619v | *Anal. Chem.* XXXX, XXX, XXX–XXX

Due to the potential significant roles of G4s in biological systems, great efforts have been made to develop G4 ligands in the past decade,[19] as well as optical probes for G4s and even G4s with specific structure.[20−26] Recently, the long wavelength (near-infrared) fluorescent probes have attracted much interest in applications of diagnosis and analysis because of low photodamage to biological samples, deep tissue penetration, and minimum interference from autofluorescence of biomolecules.[27] However, among the reported probes that have high selectivity to G4s over duplex DNA, only a very few of probes exhibit strong absorption and emission bands above 650 nm, such as porphyrin and phthalocyanine derivatives (TMPyP4,[28] Cu(TMe_2D_4),[29] PPIX,[23] and Zn-DIGP[20,30]).

Squaraines are a class of long wavelength cyanine dyes bearing a central electron deficient four-membered ring core attached by electron rich aromatic moieties.[31] These dyes exhibit sharp and intense absorption in the red to NIR region, strong fluorescence emission,[32−34] and considerable photostability.[35,36] In recent years, squaraine dyes have been extensively applied in photoconductors, optical data storage, optoelectronic devices,[37] and photodynamic therapy,[38,39] and as fluorescent probes/labels in biological applications.[40,41] Although many other cyanine dyes are widely used as fluorescent probes for nucleic acids, including G4s,[42] such as thiazole orange (TO) derivatives,[43] SYBR Green, and ETC (an extended aromatic cyanine dye),[44] squaraine dyes are rarely reported to have the optical response to nucleic acids, except in the case of a recent paper published by Zhou et al.[45]

Herein, we describe the optical response of two new squaraine dyes (STS and CSTS, Scheme 1) to different kinds of DNA. A dicyanomethylene-substituted squaraine dye, CSTS, exhibits significant absorption changes and great fluorescence enhancement in the presence of parallel G4s. The interaction mechanism of CSTS toward parallel G4s is discussed.

Scheme 1. Structures of CSTS and STS[a]

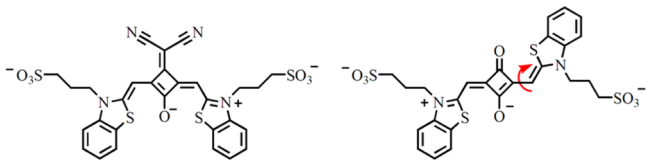

[a]CSTS possesses a cis-arrangement of the benzothiazole moieties because of congestion of dicyanomethylene group. STS experiences little steric congestion in the trans-arrangement of the benzothiazole moieties.

EXPERIMENTAL SECTION

Oligonucleotides and Squaraine Dyes. All oligonucleotides were purchased from Sunbiotech Co., Ltd. (Beijing, China). All the oligonucleotides were dissolved in Tris-HCl buffer (K^+) (10 mM Tris-HCl, 100 mM KCl, 0.1 mM EDTA pH = 7.4) except for 22AG (Na^+). 22AG (Na^+) was dissolved in Tris-HCl buffer (Na^+) (10 mM Tris-HCl, 100 mM NaCl, 0.1 mM EDTA, pH = 7.4) to form an antiparallel G4 structure. The concentration of oligonucleotides was determined based on their absorbance at 260 nm. Before testing, all oligonucleotides were heat denatured at 95 °C for 10 min followed with rapidly cooling to 4 °C and kept at this temperature overnight. dsDNA was prepared by heat denaturing and annealing the mixture of ssDNA1 and ssDNA2 (1:1). The synthesis of STS and CSTS is described in detail in the Supporting Information. Stock solutions of CSTS and STS (10 mM) were prepared in DMSO.

Absorption Spectral Titrations. Absorption spectral titrations of CSTS and STS with oligonucleotides were performed in Tris-HCl buffers mentioned above. A concentration of 4 μM CSTS was mixed with different concentrations of DNA (0, 1.0, 3.0, 4.0, 6.0, 8.0, 10, 12, 16, and 20 μM), and after standing for 30 min at room temperature in the dark the absorption spectra were collected.

Fluorimetric Titrations. Fluorimetric titrations of CSTS and STS with oligonucleotides were performed in Tris-HCl buffers mentioned above. The concentration of CSTS and STS was fixed at 4 μM. For CSTS, the concentration of oligonucleotides was 0, 1.0, 3.0, 4.0, 6.0, 8.0, 10, 12, 16, and 20 μM; for STS, the concentration of oligonucleotides was 0, 2.0, 4.0, 8.0, 12, 16, and 20 μM. After standing for 30 min at room temperature in the dark, the fluorescence spectra were collected with excitation at 680 nm (for CSTS) or 640 nm (for STS).

Curve Fitting and K_d Calculation. The data from the spectral titrations were analyzed according to the independent-site model[46] by nonlinear fitting to eq 1 or 2.[47] The parameters P and M, Q and N were found via the Levenberg−Marquardt fitting routine in the Origin 8.5 software, whereas n was varied to obtain a better fit. $K_d = Ka^{-1}$.

$$A/A_0 = 1 + \frac{P-1}{2}[M + 1 + x - \sqrt{(M+1+x)^2 - 4x}] \quad (1)$$

where A_0 is the absorption intensity of CSTS at 685 nm in the absence of DNA, A_{max} is the absorption intensity upon saturation of DNA, $P = A_{max}(A_0)^{-1}$, $M = (K_aC_{dye})^{-1}$, and $x = nC_{DNA}(C_{dye})^{-1}$.

$$F/F_0 = 1 + \frac{Q-1}{2}[N + 1 + x - \sqrt{(N+1+x)^2 4x}] \quad (2)$$

where F_0 is the fluorescence intensity of CSTS (710 nm) and STS (675 nm) in the absence of DNA, F_{max} is the fluorescence intensity upon saturation of DNA, $Q = F_{max}(F_0)^{-1}$, $N = (K_aC_{dye})^{-1}$, and $x = nC_{DNA}(C_{dye})^{-1}$.

Measurement of Fluorescent Quantum Yield (Φ). Φ values of CSTS and STS in the presence of DNA were calculated using rhodamine 800 in ethanol as standard (Φ = 0.21). Absorption intensities were recorded at 620 nm with a concentration of 10 μM of CSTS, STS, or rhodamine 800; oligonucleotides preannealed in buffer as mentioned above were added to 10 μM CSTS or STS solution to a final concentration of 70 μM. For fluorescence measurement, all samples including rhodamine 800 were diluted 20-fold, and emission spectra of 0.5 μM CSTS, STS, and rhodamine 800 were recorded from 640 to 850 nm with excitation at 620 nm. Quantum yield values were calculated according to eq 3:

$$\Phi_{sample} = \Phi_{ref}(A_{sample}/A_{ref})(OD_{ref}/OD_{sample})(n_{sample}/n_{ref})^2 \quad (3)$$

where Φ_{ref} is the quantum yield of the reference; A_{sample} and A_{ref} are the area underneath the emission spectra of the sample and the reference, respectively; and OD_{ref} and OD_{sample} are the absorbance of the reference and the sample, respectively,

dx.doi.org/10.1021/ac501619v | Anal. Chem. XXXX, XXX, XXX−XXX

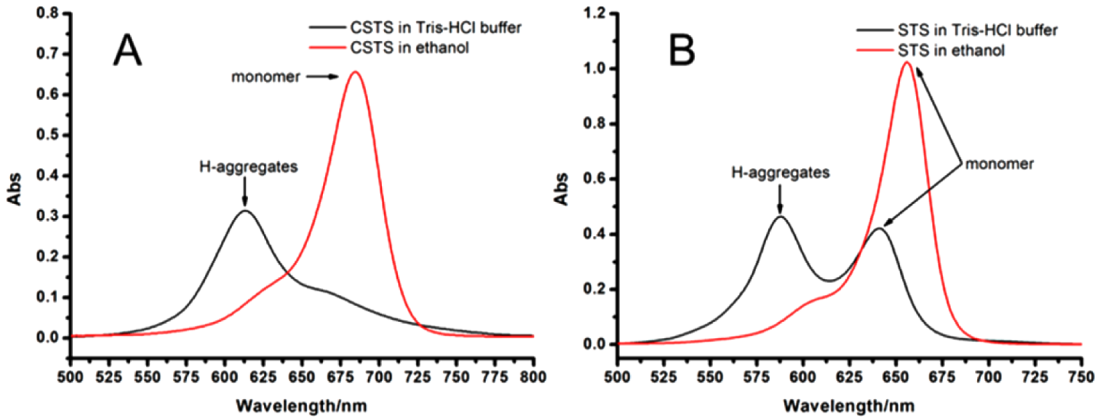

Figure 1. Absorption spectra of CSTS (A) and STS (B) in Tris-HCl buffer (K^+) and ethanol.

measured at the excitation wavelength. n_{ref} and n_{sample} are the index of refraction of the reference and the sample, respectively, in solution.

1D ^{1}H NMR Titration of G4 with CSTS. Pu22 with DMT-on was purchased from Sunbiotech Co., Ltd. (Beijing, China) and purified in our lab by RP-HPLC. After cleavage of DMT by treating with 2 mL of 80% acetic acid, the DNA sample was diluted with 1 mL of water and extracted with 10 mL of ether to remove DMT. The obtained DNA was purified again by reverse-phase HPLC and further desalted with a G-25 Sephadex NAP-5 column (GE Healthcare Life Sciences). The purified DNA was dried to a homogeneous powder. The concentration of Pu22 used for NMR testing was 200 μM. DNA samples were dissolved in 0.5 mL of 120 mM potassium phosphate buffer containing 10% D_2O, pH = 7.4, annealed by heating to 95 °C for 15 min, and then rapidly cooling to room temperature. CSTS stock solutions (10 mM) were prepared in H_2O/D_2O (9/1) solution.

Docking Process and Calculation of Binding Energy. Molecular docking on G4s (Pu22, c-kit2 and c-kit87up) was performed using Sybyl X 1.1 program (Tripos Inc.). The crystal structures of monomeric parallel-stranded DNA tetraplex were collected from PDB under codes 2KQH (c-kit2), 2O3M (c-kit87up) and 2L7V (Pu22). All of the hydrogen atoms and charges were added to define the correct configuration and tautomeric states. After extracting the binding ligands, the docking pockets were generated based on the "Ligand mode" and "residue mode", respectively. Then, the structure of the compound CSTS built by the Sybyl program was docked into the binding pockets for docking-scoring analysis. All the visual binding models created by PyMOL.

RESULTS AND DISCUSSION

Design and Synthesis of CSTS and STS. Squaraine dyes were chosen to develop the G4 probes due to their strong absorption and emission in red to NIR region, as well as good photostability.[35,36] These dyes are usually synthesized by a condensation reaction of squaric acid or its derivatives with electron rich aromatic, heteroaromatic, or olefinic compounds.[31,32,48] Since benzothiazole is an important unit in many nucleic acid binders, such as TO, SYBR Green, ETC, and so forth,[49] it was chosen as the electron-donating aromatic heterocycle for squaraine synthesis in this study (Scheme S1, Supporting Information). To increase the water solubility, propane-1-sulfonate was linked to the nitrogen atom of benzothiazole. A squaraine dye, STS, was synthesized for investigation (Scheme S1).

Recently, the V-shaped bisquinolinium,[50] bisindole,[51] and bisbenzimidazole derivatives[52,53] linked by a pyridine, benzene, or carbazole were reported to have good selectivity toward G4s over duplex DNA. Compared to the V-shaped isomer, the linear isomer of these derivatives exhibits much weaker affinity and selectivity,[54] suggesting that the V-shaped planar core is crucial for G4 recognition. As shown in Scheme 1, the conventional symmetrical squaraine like STS is a bisbenzothiazole derivative linked by squaric acid, which can adopt both trans- and cis-arrangements of the benzothiazole moieties. The dicyanomethylene substituted squaraines have been reported to adopt a cisoid conformation because of the increased sterical congestion resulting from the dicyanomethylene group. These squaraines with cisoid conformation appear to have a rigid planar π scaffold, in which a quite large open space in the vicinity of the dicyanomethylene group accommodates the substituents of the aromatic heterocycle moieties without steric congestion.[32,33] Additionally, the dicyanomethylene substituted squaraines have been reported to have excellent optical properties, such as longer ex/em wavelengths and high fluorescence quantum yields.[31−33] Since this rigid planar π scaffold of dicyanomethylene substituted squaraines is more like the V-shaped planar structure of the above-mentioned examples, it is expected that the dicyanomethylene substituted squaraines have good selectivity to the G-quadruplex. Therefore, a dicyanomethylene substituted STS was also synthesized for this investigation (Scheme S1).

Absorption and Fluorescence Spectra of CSTS and STS. It is well-known that most cyanine dyes self-aggregate in aqueous solution via van der Waals forces and $\pi-\pi$ stacking interaction, and form H- or J-type aggregates depending on the structural features of dyes as well as on the solvents or adding ions. Usually, the J-aggregates exhibit red-shifted absorption and efficient fluorescence emission (compared with monomer), and H-aggregates show blue-shifted absorption and poor emission.[44,55] Both H- and J-type aggregates of squaraines have been reported in many papers.[32,34,56] The self-aggregation behavior of CSTS and STS in Tris-HCl buffer and ethanol was investigated by absorption spectra.

As shown in Figure 1, both CSTS and STS mainly exhibited a sharp and intense absorption band with a maximum at 685 and 656 nm in ethanol, which indicates the presence of monomeric form of CSTS and STS. The molar absorption coefficients of STS and CSTS monomer were calculated to be

dx.doi.org/10.1021/ac501619v | Anal. Chem. XXXX, XXX, XXX−XXX

$\varepsilon_{650\ nm}$ = 2.37 × 10^5 mol^{-1}·L·cm^{-1} and $\varepsilon_{685\ nm}$ =1.65 × 10^5 mol^{-1}·L·cm^{-1}, respectively (Figure S1). In Tris-HCl buffer (K^+), CSTS showed a main absorption band around 613 nm and a shoulder near 650−700 nm; and STS showed two absorption bands around 588 and 641 nm. The short-wavelength bands could be assigned to the H-aggregate form; the shoulder band of CSTS and the long-wavelength band of STS could be assigned to the monomeric form. These results suggest that CSTS mainly exists in H-aggregate form and STS coexists in H-aggregate and monomer forms in Tris-HCl buffer. Increasing the concentration of K^+ or Na^+ (from 0 to 100 mM) in Tris-HCl buffer decreased both the H-aggregate and the monomer absorption bands of CSTS, suggesting that the CSTS might transform from dimer to higher H-aggregate state (Figure S2A, B). The addition of K^+ or Na^+ (from 0−100 mM) into Tris-HCl buffer increased the H-aggregate absorption band and decreased the monomer absorption band of STS, suggesting the transformation from monomer to H-aggregates (Figure S2C, D). There is no notable difference between the effects of K^+ or Na^+ on the aggregation of CSTS and STS. Both CSTS and STS exhibited strong fluorescence emission in ethanol, and the fluorescent quantum yields (Φ) were measured to be 0.47 and 0.49, respectively (Table S1). However, in Tris-HCl buffer (K^+), CSTS almost did not show fluorescence emission (Φ = 0.01), suggesting that the fluorescence was quenched by aggregation. STS in Tris-HCl buffer (K^+) exhibited weak fluorescence emission (Φ = 0.09) that was contributed to the emission from STS monomer. This set of results suggests that CSTS has a much greater tendency to form H-aggregates than STS in aqueous condition, which may be related to the rigid planar π scaffold of CSTS.

Effects of DNA on the Absorption Spectra of CSTS and STS. To investigate the interaction of CSTS and STS with different DNA, their absorption spectra in the presence of different kinds of DNA were investigated. The DNA (Table 1) includes two single-stranded DNA (ssDNA1, and its complementary sequence ssDNA2), a duplex sequence formed by ssDNA1 and ssDNA2 (dsDNA), three propeller parallel structure G4s (EAD,[57] Pu22,[58] c-kit2[59]), a snap-back parallel G4 (c-kit87up[60]), two antiparallel G4s (thrombin binding aptamer TBA[61] and 22AG(Na^+)[62]), and a mixed type G4 (22AG(K^+)[63]). Among them, 22AG is a G4-forming sequence mimicking the human telomeric repeat, which can form different type G4 structures depending on the buffer condition.[62]

Table 1. Oligonucleotides Used in This Study

name	oligonucleotide sequence (from 5′ to 3′)	G4 structure[a]
EAD	CTGGGTGGGTGGGTGGGA	intramolecular parallel
Pu22	TGAGGGTGGGTAGGGTGGGTAA	intramolecular parallel
c-kit2	CGGGCGGGCGCGAGGGAGGGT	intramolecular parallel
c-kit87up	AGGGAGGGCGCTGGGAGGAGGG	snap-back parallel
22AG(Na^+)	AGGGTTAGGGTTAGGGTTAGGG	intramolecular antiparallel
22AG(K^+)	AGGGTTAGGGTTAGGGTTAGGG	mixed type/ hybrid
TBA	GGTTGGTGTGGTTGG	intramolecular antiparallel
ssDNA1	CCAGTTCGTAGTAACCC	single stranded
ssDNA2	GGGTTACTACGAACTGG	single stranded
dsDNA	ssDNA1 + ssDNA2	double stranded

[a]G4 structures were confirmed by CD spectra (Figure S3).

As shown in Figure 2A, the addition of parallel G4s (EAD, Pu22, c-kit2, and c-kit87up) into 4 μM CSTS caused significant color loss, and other DNA did not cause noticeable color change, suggesting that CSTS could serve as a colorimetric probe for parallel G4s. The absorption spectra of CSTS showed that the monomer band increased and H-aggregate band decreased with increasing the concentration of EAD (Figure 2B), indicating the transformation from aggregated species to monomer species induced by EAD. The two well-defined isosbestic points at 640 and 728 nm indicate the equilibrium between aggregated species to monomer species. Similar spectral change was also observed in the absorption spectral titration experiments with other parallel G4s (Pu22, c-kit2, and c-kit87up) (Figure S4). However, other DNA including mixed type G4, antiparallel G4s, ssDNA, and dsDNA did not cause noticeable absorption spectral change that reflects the transformation between two species (Figure S4). The titration curves (absorbance enhancement at 685 nm against the ratio of DNA to CSTS) of CSTS with different DNA showed that CSTS has excellent selectivity to parallel G4s (EAD, Pu22, c-kit2, and c-kit87up) (Figure 2C). A 2:1 binding stoichiometry (CSTS/DNA) was revealed by fitting the data of EAD, Pu22, and c-kit2 to an independent-site model (eq 1, Experimental Section). The apparent dissociation constants (K_d) between CSTS and parallel G4s were calculated to be 8.93 μM (EAD), 15.6 μM (Pu22) and 19.7 μM (c-kit2). It is surprise that the addition of parallel G4s did not cause significant change of the absorption spectra of STS (Figure 2D and Figure S5), which suggests that parallel G4s cannot induce more H-aggregates of STS to transform to monomer form. Other DNA did not cause noticeable spectral change of STS either (Figure S5).

Effects of DNA on the Fluorescence Spectra of CSTS and STS. To further investigate the interaction of CSTS and STS with parallel G4s, the fluorescence spectra of them were collected in the presence of different concentrations of DNA. The fluorescence emission of both CSTS and STS in buffer was gradually enhanced upon the addition of parallel G4s (Figure 3A, B and Figure S6) and accompanied by a red-shift of the spectra, indicating the interaction occurred with parallel G4s. Through fitting the data to an independent-site model (eq 1, Experimental Section; Figure S7), the apparent K_d values of CSTS to G4s were estimated to be 6.57 μM (EAD), 21.6 μM (Pu22), and 9.38 μM (c-kit2), and the apparent K_d values of STS to G4s were 48.3 μM (EAD), 1379 μM (Pu22), and 107 μM (c-kit2). These data indicate that the interaction of CSTS with parallel G4s was much stronger than that of STS.

The fluorescence quantum yields (Φ) of CSTS and STS (0.5 μM) in the presence of 7-fold excess of DNA were further measured to evaluate the interaction of CSTS and STS with DNA (Figure 3C and Table S1). The quantum yields of CSTS greatly increased in the presence of parallel G4s (EAD, Pu22, c-kit2, and c-kit87up); and that of STS also increased in the presence of EAD, Pu22, and c-kit2. However, the increase extent was much lower than that of CSTS, indicating that the interaction between CSTS and parallel G4s was much stronger than that of STS. The presence of other DNA did not significantly increase the quantum yields of CSTS and STS, suggesting no or very weak interaction between these DNA and CSTS or STS. Although the fluorescence of CSTS was almost totally quenched in buffer, it almost could be restored to the level of it in ethanol by the addition of parallel G4s (EAD,

dx.doi.org/10.1021/ac501619v | Anal. Chem. XXXX, XXX, XXX−XXX

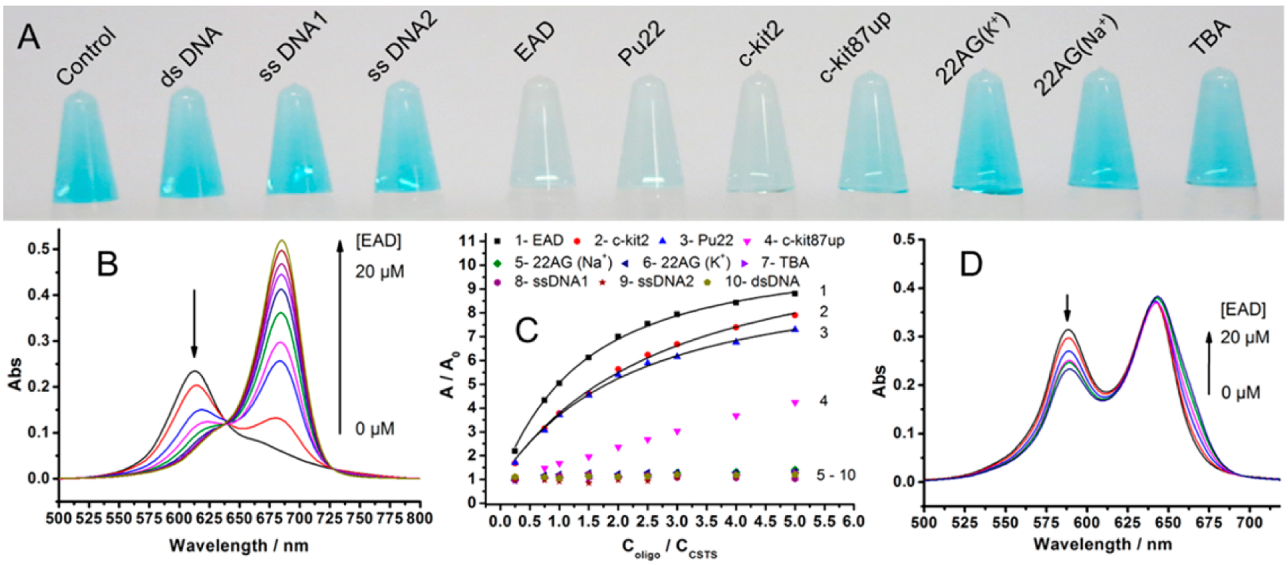

Figure 2. (A) Photograph of 10 μM CSTS interacted with different kinds of oligonucleotides in Tris-HCl buffer. Control panel is 10 μM CSTS without oligonucleotides; concentration of all oligonucleotides was fixed at 50 μM. (B) Absorption spectra of 4 μM CSTS titrated with EAD in Tris-HCl buffer (K^+); concentrations of EAD were 0, 1.0, 3.0, 4.0, 6.0, 8.0,10, 12, 16, and 20 μM. (C) Plot of absorbance enhancement of 4 μM CSTS at 685 nm against the ratio of [DNA]/[CSTS]. (D) Absorption titration spectra of 4 μM STS with EAD in Tris-HCl buffer (K^+); concentrations of EAD were 0, 4.0, 8.0, 10, 16, and 20 μM.

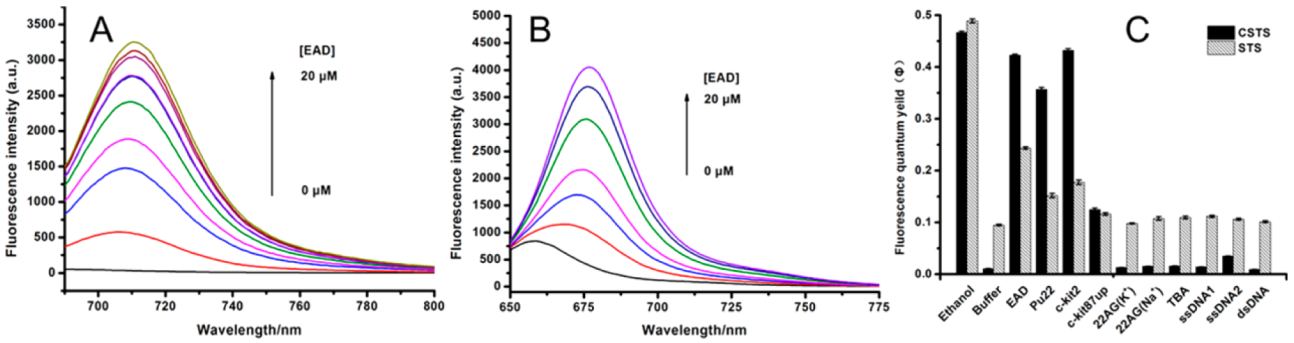

Figure 3. Fluorescence titration spectra of CSTS (A) and STS (B) with EAD. The concentration of CSTS and STS was 4 μM, and the concentration of EAD was 0, 1.0, 3.0, 4.0, 6.0, 8.0, 10, 12, 16, 20 μM (A) and 0, 2.0, 4.0, 8.0, 12, 16, 20 μM (B). (C) Fluorescence quantum yields of CSTS and STS in ethanol and buffer, and in the presence of 7-fold of different kinds of oligonucleotides. DNA was dissolved in Tris-HCl buffer as mentioned in the Experimental Section.

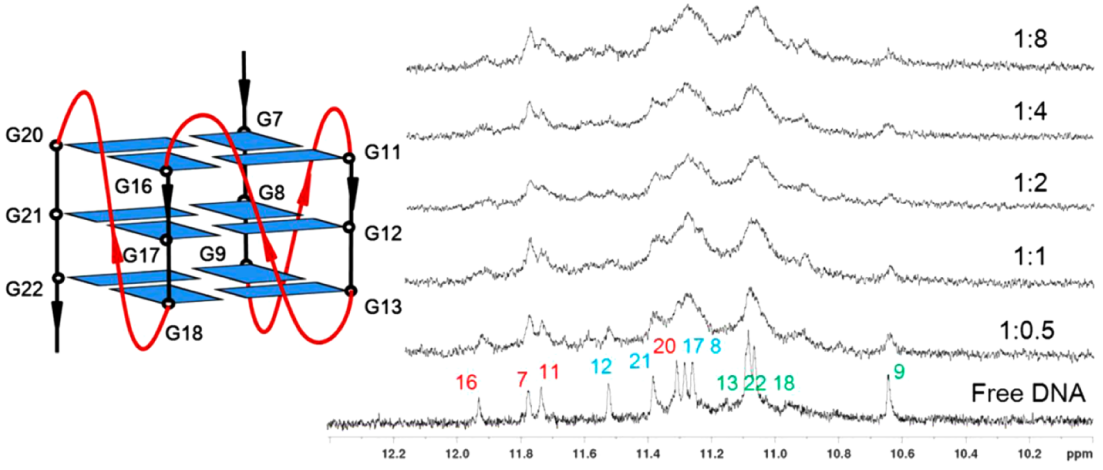

Figure 4. Imino proton regions of the 1D ^{1}H NMR titration spectra of Pu22 with CSTS in 120 mM potassium phosphate buffer, pH = 7.4. The assignments of imino protons of the free Pu22 DNA[58,64] are shown above the spectra. The imino protons from the 5′ G-tetrad are colored in red, the middle G-tetrad in blue, and the 3′ G-tetrad in green.

dx.doi.org/10.1021/ac501619v | Anal. Chem. XXXX, XXX, XXX−XXX

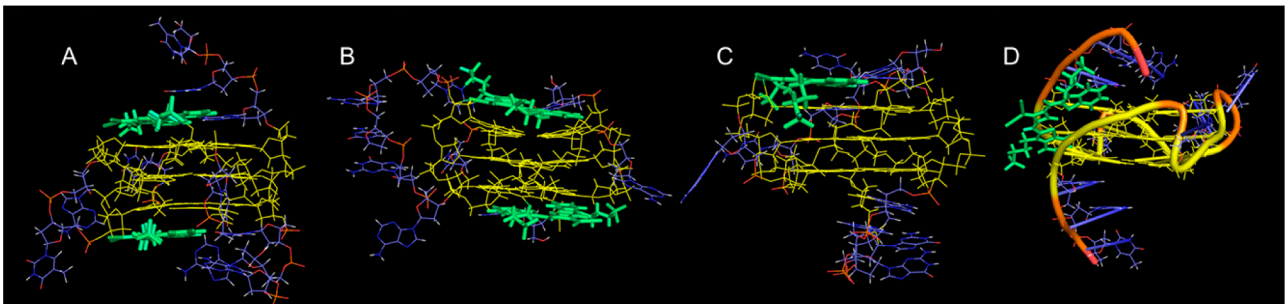

Figure 5. Binding models of CSTS to G4s. End stacking model: (A) Pu22 (PDB ID 2L7V), (B) c-kit2 (PDB ID 2KQH), and (C) c-kit87up (PDB ID 2O3M). CSTS is shown in sticks and colored by green. (A–C) G4s are shown in lines and colored by yellow (guanines) and multiple colors (other nucleotides). Groove binding model (D) of Pu22 (PDB ID 2L7V) is shown in ribbon form and colored by yellow (guanines) and multiple colors (other nucleotides).

Pu22, and c-kit2), which suggests that CSTS can serve as a light-up fluorescent probe for parallel G-quadruplex recognition.

Taken together with the results of absorption and fluorescence spectral experiments, it can be concluded that the monomer form of CSTS and STS interacts with parallel G4s, which induce the fluorescence enhancement of both dyes in buffer. The interaction force of monomeric CSTS with parallel G4s is strong enough to compete with the driving force of aggregate formation, and thus, it can induce the transformation of CSTS from aggregate form to monomer form and result in the absorption spectral change. The interaction of monomeric STS with parallel G4s could be educed from the fluorescence enhancement of STS, but the interaction force is too weak to transform more aggregates to monomers although the tendency of aggregate formation of STS in buffer is weaker than that of CSTS.

Determination of Binding Model. The interaction of CSTS with G4s was further confirmed by ^{1}H NMR titration. Guanines in the tetrads of G-quadruplex exhibit characteristic signals of chemical shifts around 10.5–12 ppm, which are assigned to the imino protons in Hoogsteen hydrogen bonding.[8,64] Therefore, the signals of these imino protons of G-quadruplex guanines provide a direct evidence for not only the formation of a G-quadruplex structure but also its drug binding interactions. As shown in Figure 4, the free DNA Pu22 exhibited 12 well-resolved imino proton peaks, as reported previously by Yang and co-workers.[58,64] These peaks broadened with the addition of CSTS up to 2 equiv, suggesting the interaction occurred between CSTS and G-tetrads. The imino proton signals of G9, G12, and G16 were found to greatly decrease with the addition of CSTS, implying the direct interaction near these G bases.

There are several binding models of G4 interaction with organic ligands, such as end-stacking and groove binding. Usually the end-stacking interactions on parallel G4s are more feasible.[65] To confirm whether CSTS binds to parallel G4s mainly by end-stacking, an inhibition experiment on the G4/hemin peroxidase activity by CSTS was performed.[66] Hemin is regarded to bind to G4 DNA by end-stacking and consequently possesses catalytic activity on the oxidation of $ABTS^{2-}$ by H_2O_2. If a candidate ligand binds at the same site as hemin on G4s, it will compete with hemin for G4 binding and decrease the rate of catalytic oxidation of G4/hemin peroxidase. Two representative parallel G4s (Pu22 and EAD) were chosen to evaluate the inhibition activity of CSTS and STS on G4/hemin peroxidase. As we expected, the addition of CSTS strongly restrained the absorbance increase at 414 nm (oxidized product of $ABTS^{2-}$) (Figure S8), suggesting that CSTS inhibited the activity of EAD/hemin and Pu22/hemin peroxidases. This result indicates that CSTS bound at the same site as hemin on G4s, that is, the end G-quartets of G4s (end-stacking). However, the addition of STS did not significantly change the peroxidase activities of EAD and Pu22 (Figure S8), suggesting that STS could not effectively compete with hemin for G4 binding, which can be attributed to the low affinity of STS to G4s.

The effect of CSTS on the conformation of G4s was investigated by measuring the CD spectra of G4s in the absence and presence of CSTS. The addition of CSTS to G4 solutions did not cause significant change of CD spectra of EAD, Pu22, c-kit2, c-kit87up, 22AG(Na^+), 22AG(K^+), and TBA (Figure S3), indicating that the binding of CSTS did not cause the change of the G-tract orientation of these G4s.

A molecular docking study was performed to understand the binding of CSTS to G4s by using Sybyl X 1.1 program (Tripos Inc.). As shown in Figure 5 and Figure S9, CSTS could bind on both ends of Pu22 and c-kit2 with relatively high scores (Pu22: top 7.47, bottom 6.27; c-kit-2: top 6.76, bottom 6.03). But for c-kit87up, CSTS only bound on the top G-quartet, and the docking score was 5.82. Because a long loop (5 nucleotides) (Figure 5C) was near the bottom of c-kit87up, it resulted in significant steric hindrance preventing CSTS end-stacking on the bottom G-quartet. The docking scores were consistent with the binding ability of CSTS to these G4s. Since small molecules may also bind to DNA in the minor groove, the docking-scoring analysis was also performed with the groove binding model. Binding pockets were generated at the grooves of the crystal structure of the Pu22 (PDB ID 2L7V), and CSTS was docked into these pockets for docking-scoring analysis. Under this condition, the obtained docking scores were from 3.19 to 3.97, which are much lower than that of the end-stacking model. This result suggests that the end-stacking mode for CSTS binding is favored over the groove binding model.

DISCUSSION

Supramolecular assemblies have been considered to be one of promising strategies for the optical probe design because of their sensitive signals changes induced by variation of assembly states.[67] Using this strategy, Huang et al.[49] have studied the interactions of compounds based on fusion of thiazole orange and isaindigotone skeleton toward different kinds of DNA, and developed a colorimetric indicator for label-free visual detection of G4s over single stranded and duplex DNA. Yang and co-

dx.doi.org/10.1021/ac501619v | Anal. Chem. XXXX, XXX, XXX–XXX

workers[44,55] have reported that parallel and antiparallel G4s could strongly interact with ETC (polymethine cyanine) monomer and disassemble ETC J-aggregates. Our results have shown that CSTS has excellent selectivity to parallel G4s, especially to the conventional propeller parallel G4s over to antiparallel G4s and mixed type G4s, as well as ss- or dsDNA. The interaction between parallel G4s and CSTS caused the disassembly of H-aggregates of CSTS, which resulted in decline and growth of the absorption peak of H-aggregates and monomeric peak, as well as the blue color vanishing (the absorption of monomer shows no visible color). The binding to parallel G4s provides CSTS a hydrophobic environment, which restores the fluorescence emission that is almost totally quenched in the aggregated form. The dicyanomethylene substitution causes a significant red-shift of the absorption and emission bands of CSTS, which makes the emission peak of CSTS longer than 700 nm. The high selectivity, long ex/em wavelengths, very low background fluorescence, large absorption coefficient, and high fluorescence quantum yield make the dicyanomethylene-functionalized squaraine hold great promise for parallel G4 detection in biological samples or in vivo. The in vivo application of one probe is determined by many factors including cell permeability, cellular location, and selectivity to G4s over other components in cells. The ongoing investigation on the dicyanomethylene-functionalized squaraine is focusing on these issues in our lab.

Unlike other cyanine dyes, squaraine dyes are rarely reported as optical probes for nucleic acid study. Most recently, after we finished this study, Zhou et al. reported that TSQ1 (a squaraine dye similar to STS) shows fluorescence enhancement selectivity to different kinds of G4s against duplex DNA.[45] Our results have shown that CSTS has much higher affinity to parallel G4s than STS, which can attribute to the V-shaped cisoid conformation of CSTS. This rigid planar π scaffold of CSTS not only enhances the end-stacking interaction with parallel G4s, but also benefits to the $\pi-\pi$ stacking between two CSTS molecules that caused the formation of H-aggregates and the quenching of fluorescence. The weak binding affinity of STS may attribute to the trans- and cis-arrangements of STS, in which the trans-arrangements conformation may not fit the G-quartet surface just like the linear bisbenzimidazole derivatives.[54] Additionally, the substitution of dicyanomethylene moiety on the central four-membered ring of squaraine may extend the conjugation of the π scaffold of CSTS, which may also benefit the $\pi-\pi$ stacking with the G-quartet surface. Intramolecular G4 formation requires three loops to link the G-tetrads. It is well-known that the loops of propeller parallel G4s distribute on the side faces of the G4s, which is in favor of the end-stacking of CSTS. For antiparallel G4s and other type of G4s, all the loops or at least one loop distribute on the top and bottom surfaces, which obstruct the stacking of CSTS on the end G-quartet surfaces. That is why CSTS showed good selectivity to parallel G4s, especially propeller parallel G4s over to other types of G4s. The different affinities of CSTS to parallel G4s may due to the different steric hindrances cause by their different loop structure and their terminal nucleotides. Among the tested parallel G4s (EAD, Pu22, c-kit2, and c-kit87up), c-kit87up showed weaker interaction than others, which may due to its snap-back loop orientation[60] that is different from the case of conventional propeller parallel G4s. These findings would provide valuable information for the design of G4 probes.

CONCLUSION

In summary, two squaraine dyes, STS and CSTS, were designed and synthesized for specific G4 recognition. The absorption spectral assay showed that CSTS was mainly present in H-aggregates in aqueous condition and STS was present in both H-aggregates and monomers. The addition of parallel G4s caused the transformation of CSTS from aggregates to monomers, but did not cause the significant transformation of STS. The fluorescent spectral assay showed that parallel G4s could enhance the fluorescence of both STS and CSTS, but the fluorescence enhancement of CSTS was much higher than that of STS, indicating the higher affinity of CSTS to parallel G4s. The ^{1}H NMR titration, G4/hemin peroxidase inhibition experiments, and molecular docking studies suggest that CSTS bound to G4s through end-stacking on G-quartet surface. The dicyanomethylene substitution in CSTS makes it adopt a cisoid conformation; this V-shaped conformation was considered to contribute to the high selectivity of CSTS to parallel G4s. The excellent selectivity to parallel G4s and the advantageous optical properties of squaraine dye allow CSTS to serve as a light-up fluorescent probe to discriminate propeller parallel G4s from other DNA forms in biological samples or in vivo.

ASSOCIATED CONTENT

Supporting Information

Additional information as noted in the text. This material is available free of charge via the Internet at http://pubs.acs.org

AUTHOR INFORMATION

Corresponding Author

*Tel/Fax: 86-10-62528509. E-mail: sgdh@iccas.ac.cn.

Notes

The authors declare no competing financial interest.

ACKNOWLEDGMENTS

We gratefully acknowledge the financial support from Grant 973 Program (2011CB935800, 2013CB933700, and 2011CB911000) and NSF of China (21275149, 21375135, and 21321003).

REFERENCES

(1) Burge, S.; Parkinson, G. N.; Hazel, P.; Todd, A. K.; Neidle, S. *Nucleic Acids Res.* **2006**, *34*, 5402−5415.
(2) Davis, J. T. *Angew. Chem., Int. Ed.* **2004**, *43*, 668−698.
(3) Huppert, J. L.; Balasubramanian, S. *Nucleic Acids Res.* **2007**, *35*, 406−413.
(4) Eddy, J.; Maizels, N. *Nucleic Acids Res.* **2008**, *36*, 1321−1333.
(5) Huppert, J. L.; Bugaut, A.; Kumari, S.; Balasubramanian, S. *Nucleic Acids Res.* **2008**, *36*, 6260−6268.
(6) Xu, Y. *Chem. Soc. Rev.* **2011**, *40*, 2719−2740.
(7) Phan, A. T.; Modi, Y. S.; Patel, D. J. *J. Am. Chem. Soc.* **2004**, *126*, 8710−8716.
(8) Waller, Z. A. E.; Sewitz, S. A.; Hsu, S. T. D.; Balasubramanian, S. *J. Am. Chem. Soc.* **2009**, *131*, 12628−12633.
(9) Paramasivam, M.; Membrino, A.; Cogoi, S.; Fukuda, H.; Nakagama, H.; Xodo, L. E. *Nucleic Acids Res.* **2009**, *37*, 2841−2853.
(10) Sun, D. Y.; Guo, K. X.; Rusche, J. J.; Hurley, L. H. *Nucleic Acids Res.* **2005**, *33*, 6070−6080.
(11) Palumbo, S. L.; Memmott, R. M.; Uribe, D. J.; Krotova-Khan, Y.; Hurley, L. H.; Ebbinghaus, S. W. *Nucleic Acids Res.* **2008**, *36*, 1755−1769.
(12) Lew, A.; Rutter, W. J.; Kennedy, G. C. *Proc. Natl. Acad. Sci. U.S.A.* **2000**, *97*, 12508−12512.

(13) Balasubramanian, S.; Hurley, L. H.; Neidle, S. *Nat. Rev. Drug Discovery* **2011**, *10*, 261−275.
(14) De Cian, A.; Lacroix, L.; Douarre, C.; Temime-Smaali, N.; Trentesaux, C.; Riou, J. F.; Mergny, J. L. *Biochimie* **2008**, *90*, 131−155.
(15) Maizels, N. *Nat. Struct. Mol. Biol.* **2006**, *13*, 1055−1059.
(16) Biffi, G.; Tannahill, D.; McCafferty, J.; Balasubramanian, S. *Nat. Chem.* **2013**, *5*, 182−186.
(17) Biffi, G.; Di Antonio, M.; Tannahill, D.; Balasubramanian, S. *Nat. Chem.* **2014**, *6*, 75−80.
(18) Brooks, T. A.; Kendrick, S.; Hurley, L. *FEBS J.* **2010**, *277*, 3459−3469.
(19) Ou, T. M.; Lu, Y. J.; Tan, J. H.; Huang, Z. S.; Wong, K. Y.; Gu, L. Q. *ChemMedChem* **2008**, *3*, 690−713.
(20) Alzeer, J.; Vummidi, B. R.; Roth, P. J. C.; Luedtke, N. W. *Angew. Chem., Int. Ed.* **2009**, *48*, 9362−9365.
(21) Kong, D. M.; Ma, Y. E.; Wu, J.; Shen, H. X. *Chem.—Eur. J.* **2009**, *15*, 901−909.
(22) Yang, P.; De Cian, A.; Teulade-Fichou, M. P.; Mergny, J. L.; Monchaud, D. *Angew. Chem., Int. Ed.* **2009**, *48*, 2188−2191.
(23) Li, T.; Wang, E. K.; Dong, S. J. *Anal. Chem.* **2010**, *82*, 7576−7580.
(24) Mohanty, J.; Barooah, N.; Dhamodharan, V.; Harikrishna, S.; Pradeepkumar, P. I.; Bhasikuttan, A. C. *J. Am. Chem. Soc.* **2013**, *135*, 367−376.
(25) Jin, B.; Zhang, X.; Zheng, W.; Liu, X. J.; Qi, C.; Wang, F. Y.; Shangguan, D. H. *Anal. Chem.* **2014**, *86*, 943−952.
(26) Zhang, L. Y.; Er, J. C.; Ghosh, K. K.; Chung, W. J.; Yoo, J.; Xu, W.; Zhao, W.; Phan, A. T.; Chang, Y. T. *Sci. Rep.* **2014**, *4*, 3776.
(27) Yuan, L.; Lin, W. Y.; Zheng, K. B.; He, L. W.; Huang, W. M. *Chem. Soc. Rev.* **2013**, *42*, 622−661.
(28) Han, F. X. G.; Wheelhouse, R. T.; Hurley, L. H. *J. Am. Chem. Soc.* **1999**, *121*, 3561−3570.
(29) Zhao, P.; Xu, L. C.; Huang, J. W.; Fu, B.; Yu, H. C.; Ji, L. N. *Dyes Pigm.* **2009**, *83*, 81−87.
(30) Qin, H. X.; Ren, J. T.; Wang, J. H.; Luedtke, N. W.; Wang, E. K. *Anal. Chem.* **2010**, *82*, 8356−8360.
(31) Pisoni, D. D.; Petzhold, C. L.; de Abreu, M. P.; Rodembusch, F. S.; Campo, L. F. *C. R. Chim.* **2012**, *15*, 454−462.
(32) Mayerhoffer, U.; Gsanger, M.; Stolte, M.; Fimmel, B.; Wurthner, F. *Chem.—Eur. J.* **2013**, *19*, 218−232.
(33) Mayerhoffer, U.; Fimmel, B.; Wurthner, F. *Angew. Chem., Int. Ed.* **2012**, *51*, 164−167.
(34) Wang, W. H.; Fu, A.; Lan, J. B.; Gao, G.; You, J. S.; Chen, L. J. *Chem.—Eur. J.* **2010**, *16*, 5129−5137.
(35) Keil, D.; Hartmann, H.; Moschny, T. *Dyes Pigm.* **1991**, *17*, 19−27.
(36) Wang, B. S.; Fan, J. L.; Sun, S. G.; Wang, L.; Song, B.; Peng, X. J. *Dyes Pigm.* **2010**, *85*, 43−50.
(37) Emmelius, M.; Pawlowski, G.; Vollmann, H. W. *Angew. Chem., Int. Ed.* **1989**, *28*, 1445−1471.
(38) Ramaiah, D.; Eckert, I.; Arun, K. T.; Weidenfeller, L.; Epe, B. *Photochem. Photobiol.* **2004**, *79*, 99−104.
(39) Santos, P. F.; Reis, L. V.; Almeida, P.; Serrano, J. P.; Oliveira, A. S.; Ferreira, L. F. V. *J. Photochem. Photobiol. A* **2004**, *163*, 267−269.
(40) Patonay, G.; Salon, J.; Sowell, J.; Strekowski, L. *Molecules* **2004**, *9*, 40−49.
(41) Jisha, V. S.; Arun, K. T.; Hariharan, M.; Ramaiah, D. *J. Phys. Chem. B* **2010**, *114*, 5912−5919.
(42) Largy, E.; Granzhan, A.; Hamon, F.; Verga, D.; Teulade-Fichou, M. P. *Top. Curr. Chem.* **2013**, *330*, 111−177.
(43) Peng, X. J.; Wu, T.; Fan, J. L.; Wang, J. Y.; Zhang, S.; Song, F. L.; Sun, S. G. *Angew. Chem., Int. Ed.* **2011**, *50*, 4180−4183.
(44) Yang, Q. F.; Xiang, J. F.; Yang, S.; Zhou, Q. J.; Li, Q.; Tang, Y. L.; Xu, G. Z. *Chem. Commun.* **2009**, 1103−1105.
(45) Chen, Y. Q.; Yan, S. Y.; Yuan, L. B.; Zhou, Y. M.; Song, Y. Y.; Xiao, H.; Weng, X. C.; Zhou, X. *Org. Chem. Front.* **2014**, *1*, 267−270.
(46) Stootman, F. H.; Fisher, D. M.; Rodger, A.; Aldrich-Wright, J. R. *Analyst* **2006**, *131*, 1145−1151.
(47) Xie, X.; Choi, B.; Largy, E.; Guillot, R.; Granzhan, A.; Teulade-Fichou, M. P. *Chem.—Eur. J.* **2013**, *19*, 1214−1226.
(48) Reis, L. V.; Serrano, J. P. C.; Almeida, P.; Santos, P. F. *Synlett* **2002**, 1617−1620.
(49) Yan, J. W.; Ye, W. J.; Chen, S. B.; Wu, W. B.; Hou, J. Q.; Ou, T. M.; Tan, J. H.; Li, D.; Cu, L. Q.; Huang, Z. S. *Anal. Chem.* **2012**, *84*, 6288−6292.
(50) Monchaud, D.; Yang, P.; Lacroix, L.; Teulade-Fichou, M. P.; Mergny, J. L. *Angew. Chem., Int. Ed.* **2008**, *47*, 4858−4861.
(51) Dash, J.; Shirude, P. S.; Balasubramanian, S. *Chem. Commun.* **2008**, 3055−3057.
(52) Jain, A. K.; Reddy, V. V.; Paul, A.; Muniyappa, K.; Bhattacharya, S. *Biochemistry* **2009**, *48*, 10693−10704.
(53) Li, G. R.; Huang, J.; Zhang, M.; Zhou, Y. Y.; Zhang, D.; Wu, Z. G.; Wang, S. R.; Weng, X. C.; Zhou, X.; Yang, G. F. *Chem. Commun.* **2008**, 4564−4566.
(54) Bhattacharya, S.; Chaudhuri, P.; Jain, A. K.; Paul, A. *Bioconjugate Chem.* **2010**, *21*, 1148−1159.
(55) Yang, Q. F.; Xiang, J. F.; Yang, S.; Li, Q. A.; Zhou, Q. J.; Guan, A. J.; Li, L.; Zhang, Y. X.; Zhang, X. F.; Zhang, H.; Tang, Y. L.; Xu, G. Z. *Anal. Chem.* **2010**, *82*, 9135−9137.
(56) Xu, Y. Q.; Malkovskiy, A.; Wang, Q. M.; Pang, Y. *Org. Biomol. Chem.* **2011**, *9*, 2878−2884.
(57) Cheng, X. H.; Liu, X. J.; Bing, T.; Zhao, R.; Xiong, S. X.; Shangguan, D. H. *Biopolymers* **2009**, *91*, 874−883.
(58) Dai, J. X.; Carver, M.; Hurley, L. H.; Yang, D. Z. *J. Am. Chem. Soc.* **2011**, *133*, 17673−17680.
(59) Hsu, S. T. D.; Varnai, P.; Bugaut, A.; Reszka, A. P.; Neidle, S.; Balasubramanian, S. *J. Am. Chem. Soc.* **2009**, *131*, 13399−13409.
(60) Phan, A. T.; Kuryavyi, V.; Burge, S.; Neidle, S.; Patel, D. J. *J. Am. Chem. Soc.* **2007**, *129*, 4386−4392.
(61) Martino, L.; Virno, A.; Randazzo, A.; Virgilio, A.; Esposito, V.; Giancola, C.; Bucci, M.; Cirino, G.; Mayol, L. *Nucleic Acids Res.* **2006**, *34*, 6653−6662.
(62) He, Y. J.; Neumann, R. D.; Panyutin, I. G. *Nucleic Acids Res.* **2004**, *32*, 5359−5367.
(63) Ambrus, A.; Chen, D.; Dai, J. X.; Bialis, T.; Jones, R. A.; Yang, D. Z. *Nucleic Acids Res.* **2006**, *34*, 2723−2735.
(64) Ambrus, A.; Chen, D.; Dai, J. X.; Jones, R. A.; Yang, D. Z. *Biochemistry* **2005**, *44*, 2048−2058.
(65) Boer, D. R.; Canals, A.; Coll, M. *Dalton Trans.* **2009**, 399−414.
(66) Cheng, X. H.; Liu, X. J.; Bing, T.; Cao, Z. H.; Shangguan, D. H. *Biochemistry* **2009**, *48*, 7817−7823.
(67) Liu, X. J.; Qi, C.; Bing, T.; Cheng, X. H.; Shangguan, D. H. *Anal. Chem.* **2009**, *81*, 3699−3704.